Received: 25 January 2024 | Revised: 10 April 2024 | Accepted: 10 May 2024 | Published online: 21 May 2024

RESEARCH ARTICLE

Archives of Advanced Engineering Science
2024, Vol. 00(00) 1–11
DOI: 10.47852/bonviewAAES42022525

BON VIEW PUBLISHING

Crystallization of FeC Iron Monocarbide During Peritectoidal Transformation of the Lamellar Eutectoid of Ledeburite White Eutectic Cast Iron

Sergey Vasilyevich Davydov[1,*]

[1]*Bryansk State Technical University, Russia*

Abstract: The previously unknown process of homogeneous and heterogeneous crystallization of FeC iron monocarbide and its co-crystallizations with ε-carbide Fe_2C from a supersaturated solid solution based on ε-carbide Fe_2C or polycarbide quasi-eutectic formed in the process of peritectoid decomposition during prolonged heating (isothermal annealing) of the lamellar eutectoid ledeburite in cast eutectic white iron has been investigated. Crystallization of two-dimensional monolayers of FeC monocarbide allotropes in the form of translucent extended and elastic crystalline nanofilms has been experimentally proved. The carbide phases in white cast iron can be characterized as a single isomorphic and isostructural quasi-carbide solid solution, which structurally crystallizes as a mixture of carbide phases as a quasi-eutectic, in which the carbon content is free to vary widely without identification of the carbide phases proper. The decomposition product of the lamellar eutectoid as a result of peritectoid transformation during isothermal annealing is polycarbide with a gradient crystal lattice of solid solutions corresponding in carbon concentration to this or that carbide.

Keywords: lamellar eutectoid, troostite, crystallizations, polycarbide

1. Introduction

There are no objective data on FeC monocarbide as a chemical compound [1, 2]. FeC monocarbide has not been systematically investigated and is not mentioned either in works on the FeC diagram or in general in materials science and metallurgy [3, 4]. The work of Bahgat [5] discusses various methods (gaseous carburization, mechanochemical synthesis, laser pyrolysis, plasma pyrolysis, chemical vapor deposition, ion implantation) for the synthesis of basic iron carbides (Fe_3C, Fe_7C_3, Fe_5C_2, Fe_2C); attention is also paid to the exotic carbide $Fe_{75}C_{25}$, but the synthesis of FeC iron monocarbide is not considered.

Comprehensive studies of FeC monocarbide began in a scientific discipline that has nothing to do with materials science and metallurgy – astrophysics. In the spectra of star formation and cold carbon stars in 1988, lines of FeC monocarbide and monocarbides of other elements, such as SiC, were detected. This fact was the impetus for investigating, first of all, the spectral characteristics of the FeC monocarbide molecule and its atomic and electronic structure. However, these studies had to be postponed because it was impossible to obtain FeC monocarbide by existing chemical and metallurgical technologies, and it was necessary to develop fundamentally new technologies for the synthesis of FeC monocarbide only in the form of single molecules.

The first studies of spectroscopic characteristics of FeC monocarbide molecules by resonant two-photon ionization spectroscopy were performed by Balfour et al. [6], in which FeC monocarbide was obtained as a result of the reaction of laser-vaporized iron atoms with methane in a helium atmosphere at its supersonic expansion. The electronic structure of FeC monocarbide was investigated by Shim and Gingerich [7]. In this work, the dissociation energy De of FeC monocarbide was determined to be 2.79 eV. In the work of Brugh and Morse [8], FeC monocarbide was studied by resonant two-photon ionization spectroscopy, and some new electronic states were identified, and the binding energy was determined to be 3.9 ± 0.3 eV and the ionization energy to be 7.74 ± 0.09 eV.

To obtain FeC monocarbide, Brugh and Morse [8] applied a rather complex and virtuoso technology. Initially, the production of FeC monocarbide was achieved by pulsed laser ablation of a carbon steel target disc with a power of 1–2 mJ of the second harmonic of the Nd:YAG laser in a supersonic expansion beam of 3% methane in helium, which after passing through a 3 cm channel was expanded through a 2 mm diameter hole. The mole percentage of carbon in the carbon steel sample disc was too low to produce appreciable amounts of FeC molecules in the pure helium expansion. Replacing the disc with a sample pressed from a powder consisting of iron and carbon powders in a molar ratio of 3:1 was about twice as efficient for FeC production as the carbon steel method.

In the studies of Aiuchi and Shibuya [9], FeC monocarbide was obtained by laser ablation reaction of Fe atoms with CH_4 methane, and

*Corresponding author: Sergey Vasilyevich Davydov, Bryansk State Technical University, Russia. Email: fulleren_grafen@mail.ru

its spectrum was studied using laser-induced fluorescence. In the visible region of the spectrum, it was possible to characterize five electronic states and investigate spin-orbit splitting. Spin analysis was performed for 46 vibronic bands. 35 bands were observed for the first time.

The permanent electric dipole moments of FeC monocarbide were investigated by Steimle et al. [10]. For the first time in the laboratory using direct absorption techniques in the millimeter-submillimeter range, Allen et al. [11] measured the pure rotational spectrum and investigated some spin-orbit parameters of FeC monocarbide, which was synthesized as a result of the reaction of iron vapor produced in a high-temperature Broyde-type furnace in an atmosphere of methane gas under DC discharge conditions.

The studies of FeC monocarbide, the results of which are applicable in metallurgy for the analysis of phase processes and structure formation in the Fe-Fe_3C system, have been performed relatively recently in 2016–2022 [12–15]. In these and other works, it was found that FeC monocarbide has unique properties such as superconductivity and metallic and catalytic properties in the synthesis of carbon nanotubes and in Fischer-Tropsch liquid fuel synthesis. It was found that the structure of FeC monocarbide is layered and has enormous internal capacitance, for example, for lithium atoms, which makes it possible to use FeC monocarbide as a basis in rechargeable lithium batteries.

Liu et al. [12] were the first to perform Mössbauer spectroscopy of iron carbides (α-Fe, γ'-FeC, η-Fe_2C, ζ-Fe_2C, χ-Fe_5C_2, h-Fe_7C_3, θ-Fe_3C, o-Fe_7C_3, γ'-Fe_4C, γ''-Fe_4C, and α'-$Fe_{16}C_2$) using the full-potential linearized plane wave method, which enabled the determination of the crystallographic structure of the whole line of carbides. The Mössbauer parameters of γ'-FeC, η-Fe_2C, ζ-Fe_2C, h-Fe_7C_3, o-Fe_7C_3, γ'-Fe_4C, γ''-Fe_4C, and α'-$Fe_{16}C_2$ have also been theoretically predicted. Almost single-phase χ-Fe_5C_2 and θ-Fe_3C were experimentally obtained.

Mössbauer spectroscopy of iron carbides revealed the crystallographic correspondence of the carbide structures and their stability. Depending on the places occupied by carbon atoms in the carbide crystal lattice, all these carbides can be divided into octahedral, trigonal-prismatic, and tetrahedral [12].

The octahedral carbides include γ'-FeC, α'-$Fe_{16}C_2$, η-Fe_2C, ζ-Fe_2C, and γ''-Fe_4C carbides. In addition, γ'-FeC and γ''-Fe_4C consist of γ-Fe (HCC) sublattices with octahedral interdoped C atoms. The η-Fe_2C and ζ-Fe_2C carbides have hexagonal dense packing of Fe sublattices.

The second type of carbides is the trigonal-prismatic carbides h-Fe_7C_3, o-Fe_7C_3, χ-Fe_5C_2, and θ-Fe_3C, in which C atoms are arranged in trigonal-prismatic sites of the distorted hexagonal-closed structure of Fe atoms. The last type is the tetrahedral carbide, γ'-Fe_4C.

The average distance between Fe and C atoms in these carbides is about 1.90 Å, which falls within the expected range of FeC distances for many carbide structures. The closest distance between C and C atoms varies from 2.60 Å to 3.50 Å, indicating the absence of C-C dimers in the iron carbides.

The studies [12–15] provide, to a fairly certain extent, an opportunity to further explain many important points, including the high variable percentage of carbon content in the carbide phases.

Dong et al. and others [13, 14] have performed theoretical studies of the crystallographic structure of FeC monocarbide and some thermodynamic properties for the first time, and mechanical properties have been calculated. Dong et al. and others [13, 14] by ab initio simulations (VASP) theoretically discovered energetically stable two-dimensional allotropes of FeC monocarbide characterized by planar hypercoordination chemical bonding, respectively: tetragonal FeC monocarbide (t-FeC) and orthorhombic FeC monocarbide (o-FeC).

From an energetic point of view, the t-FeC allotrope is a two-dimensional tetragonal layer in which each carbon atom is four-coordinated with the surrounding four iron atoms. The o-FeC allotrope monolayer is an orthorhombic planar phase with a pentacoordinated carbon bond and a planar seven-coordinated bond of iron atoms. The FeC monocarbide allotropes are the first example of two-dimensional monolayers with simultaneously pentacoordinated carbon bonds and semi-coordinated iron atom bonds in known iron-carbon materials. Theoretical calculations confirm that all these monolayers have significant dynamic, mechanical, and thermal stability.

Dong et al. and others [13, 14] calculated the Ecoh cohesive energies of t-FeC and o-FeC allotrope monolayers to be 5.76 and 5.59 eV/atom, respectively. The high cohesive energy is a guarantee that t-FeC and o-FeC monolayers are strongly bonded iron-carbon networks. The structure of the t-FeC monolayer can be regarded as a quasi-planar tetragonal lattice with space group P4/nmm, in which each C atom is quasi-planarly four-coordinated with the surrounding four Fe atoms. The planar monolayer of the t-FeC allotrope has a slightly corrugated square structure with a thickness of $\delta = 1.26$ Å. The lattice constants are $a = b = 3.49$ Å.

The structure of the o-FeC monolayer can be regarded as a quasi-planar orthorhombic lattice with space group Cmmm, in which each C atom is quasi-planarly coordinated with five neighboring atoms (one C atom and four Fe atoms), forming a planar five-coordinated bond, and each Fe atom is coordinated with four carbon atoms and three iron atoms, forming a planar seven-coordinated bond. Therefore, unlike the t-FeC monolayer with a corrugated structure, the o-FeC monolayer has a perfect flat lattice with thickness $\delta = 1.85$ Å. The lattice constants are $a = 5.96$ Å, $b = 4.49$ Å. This type of bonding in the monolayers of o-FeC and t-FeC allotropes determines its metallic character.

In the thesis work of the Russian scientist Larionov [15], FeC monocarbide and its allotropes o-FeC and t-FeC were also studied. The energetic favorability of the layered orthorhombic phase of FeC monocarbide was shown, and the thermodynamic stability of the orthorhombic monolayers of the o-FeC allotrope and the corrugated monolayers of the t-FeC allotrope phase was proved.

It is possible to obtain monophase FeC monocarbide, as well as other iron carbides, from ledeburite two-component (Fe + C) white cast irons of eutectic and transeutectic composition in accordance with the diagram of the state of Fe-C alloys, but this issue of research of FeC monocarbide isolated from white cast irons has not been considered so far even in theoretical terms.

Ledeburite of white cast iron or eutectic of two-component Fe-C alloy is traditionally known as a stable two-phase structure (cementite + ferrite) of white eutectic cast irrespective of their chemical composition [16–18] and is thermodynamically relatively stable to external thermal effects, except for the production of ductile cast iron [19, 20].

Recently, ledeburite has been considered either as an intermetallic compound in the structure of iron-carbon alloys, for example, as a steel of the ledeburite class in the production of Damascus steel [21], or as a natural metal-ceramic composite material. Vasyunina et al. showed [22] that according to the results of X-ray diffraction analysis, the structure of cast iron containing 93.8% Fe and 4.99% C is considered hypereutectic white cast iron with a composite structure (ledeburite + graphite).

The production of iron carbides is also possible during the heat treatment of ledeburite, as well as quenching martensite. If, during prolonged high-temperature graphitizing annealing, cementite and

ledeburite of white cast iron completely decomposes into perlite and floccular graphite, with the formation of a ductile iron structure [19, 20], then during controlled annealing, ledeburite decomposes into carbides.

Sukhanov and Arkhangelsky established [23] that in the process of isothermal annealing of high-purity two-component white cast iron (2.25%C) at 650–950°C, the process of decomposition of ledeburite into more stable eutectic carbides begins, providing technological plasticity for subsequent forging. The influence of the purity of white cast iron on the morphology of excess carbides and their ability to divide has been established. Sukhanov and Arkhangel'skii [24] also investigated the morphology of excess eutectic carbides after melting, pre-annealing, and after deformation forging. It is noted that the stoichiometric composition of faceted eutectic carbides is in the range of 34.0< C < 36.0 at.%, which corresponds to Fe_2C type ε-carbide with a hexagonal close-packed lattice. A two-stage mechanism of transformation of excess secondary cementite into faceted eutectic e-carbides of the Fe_2C type during heat treatment is considered.

The study of the decay of martensite, perlite, and quasi-perlite structures has been carried out in a number of works [25–29]. Pereira [27] showed that the two initial microstructures (perlite and lower bainite) were compared in their propensity to spheroidization by dilute eutectoid transformation during the simulation of the heat-affected zone (HAZ) thermal cycle. The kinetics of phase transformations in the heat treatment process was also analyzed using high-resolution dilatometric studies. The results showed that lower bainite has a greater tendency to spheroidize cementite than perlite due to the initial configuration of carbides. In addition, it has been confirmed that the higher the cooling rate, the lower the tendency to spheroidization.

Ribamar [28], using in situ synchrotron X-ray diffraction, contact dilatometry, scanning electron microscopy, microhardness, and atomic probe tomography, found out the mechanisms of stabilization and decay of carbon in austenite of high-carbon bearing steels (% C >0.8, the microstructure of which consists of solid hardened martensite (a't) + spheroidized cementite (Θ-Fe_3C) + a small amount of preserved austenite (γR)). This complex microstructure is achieved by quenching from inter-critical annealing (in the phase field cementite Θ-Fe_3C+γR) followed by tempering at low temperature (200–250°C). The time and temperature necessary for the effective separation of carbon into austenite or microstructural decomposition into secondary cementite have been identified.

The results obtained are discussed on the basis of various equilibrium states between martensite a't and carbides. It was found that at temperatures below 300°C, carbon stratification toward the preserved austenite occurs within a few minutes without significant phase decay. The transition temperature between the predominant enrichment of austenite with carbon and the decomposition of austenite occurs at 350°C. Secondary deposition of cementite inside martensite and at the a't/γR boundaries is observed during tempering at temperatures above 400°C. The results of carbon equilibrium modeling, taking into account the presence of carbides, show that uniformly dispersed spheroidized primary cementite has little effect on the phenomenon of carbon separation.

Carbides of the M_3C and M_7C_3 type in the microstructure of white cast irons, the composition of which depends on alloying and heat treatment mode, were studied by [30].

The performed brief review [31–33] clearly shows that the performed studies are in the traditional paradigm defined by the Fe-C alloy state diagram and, in particular, from the concept of ledeburite as a two-phase eutectic structure consisting of cementite (iron carbide Θ-Fe_3C containing 6.67%C) and ferrite (solid solution carbon in the α-Fe polymorph). In the works of the authors [31–33], a previously unknown phase transformation was discovered within the FeC diagram, as the peritectoid transformation of perlite into a polycarbide structure consisting primarily of monocarbide FeC and ε-carbide Fe_2C.

With all the helplessness of existing chemical and industrial technologies in the field of synthesis of FeC monocarbide and obtaining it in crystalline state, the authors [30–32] found that FeC monocarbide perfectly co-crystallizes in the process of peritectoid transformation [30] of lamellar eutectoid in white eutectic cast iron [31] with ε-carbide Fe_2C from supersaturated solid solution based on ε-carbide Fe_2C or polycarbide quasi-eutectic. In the development of the obtained new data [30–32], the author carried out additional studies of the fine structure of polycarbide quasi-eutectics.

2. Equipment, Materials, and Research Methodology

The present investigations were carried out on two-component (FeC) white eutectic cast iron (C = 4.3%C) of high purity, smelted in a micro-arc electric furnace according to the method [31]. Fine microstructure studies were performed on cast samples and samples that underwent prolonged isothermal annealing at 330^{0}C ± 10 ^{0}C for 36 h to complete the peritectoidal transformation of lamellar eutectoid (troostite) [30–32].

Metallographic studies were carried out on a Leica DMIRM digital optical metallographic microscope using Image Scope Color M image analysis software.

For a more detailed assessment of phase transformations and emerging structures in the process of peritectoidal transformation, the fine ledeburite structure of the lamellar eutectoid was investigated both in the cast state and after isothermal annealing using FEI Scios 2 LoVac double-beam electron microscope using DualBeam™ super-resolution analytical technology, which provides the study of fine structure in two-dimensional and three-dimensional projection. To reveal the two-dimensional surface structure of white cast iron ledeburite, we used etching with 5% nitric acid solution in alcohol (Nital) at 24^{0}C for 3–5 s. To reveal the internal three-dimensional structure of polycarbide quasi-eutectic, it was dissolved in the process of hot etching with 5% nitric acid solution in distilled water at 50^{0}C for 5–10 s (in some variants up to ~1.0 min) with subsequent washing of microdots in alcohol. As a result of the removal of eutectoid colony content during etching, an internal cavity or phase cell (working term) with inclusions of carbide phase is formed in the ledeburite skeleton (matrix). Chemical local microanalysis of the phases was performed using an X-ray vacuum spectrometer EDAX Octane Elite Plus, which uses a detector based on silicon nitride (Si_3N_4), which provides a significant improvement in sensitivity to the concentration of the determined elements.

3. Discussion of Experimental Results

The average thickness of ferrite plates in the lamellar eutectoid of ledeburite white cast iron in the cast state (Figure 1a) varies within δfer = 0.095 . . . 0.170 μm and the average thickness of cementite plates δcem = 0.015 . . . 0.055 μm. The degree of dispersity of the lamellar ferrite-cementite mixture is in the range δ = 0.110 . . . 0.225 μm, which corresponds to quasi-perlite or troostite (Figure 2a).

In the process of isothermal annealing, the peritectoidal reaction of dissolution of cementite in ferrite [30–32] with formation of supersaturated solid solution based on ε-carbide Fe_2C begins to occur in the lamellar troostite of ledeburite (Figure 2a) by the reaction: -Fe_3C (cementite) + α-Fe (ferrite) = ε-carbide Fe_2C (supersaturated solid solution).

Figure 1
Structure of lamellar eutectoid (troostite) of ledeburite in eutectic white cast iron. (a) Cast structure. (b) After completion of peritectoid transformation during isothermal holding for 36 h at 330°C ± 10°C; ×500, Nital etching

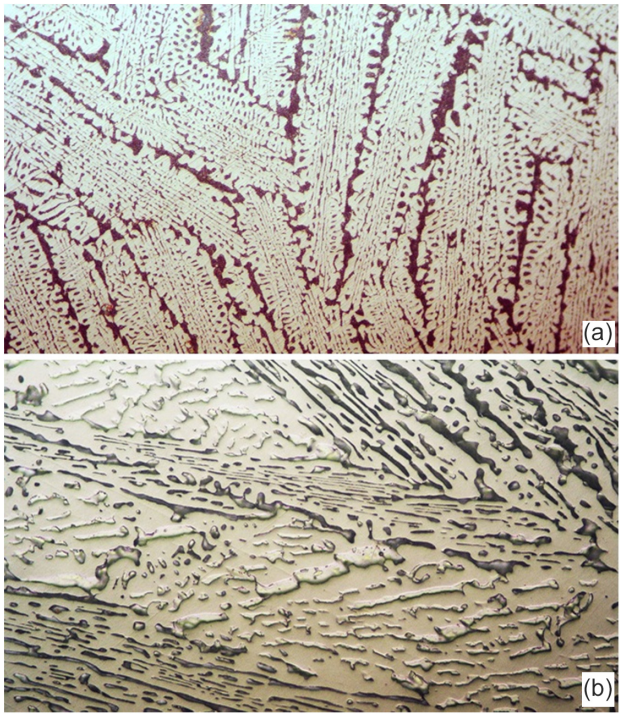

Upon completion of peritectoid transformation, the lamellar troostite of ledeburite white cast iron (Figure 2a) completely transforms into polycarbide quasi-eutectic (Figure 1b) based on a supersaturated solid solution of ε-carbide Fe_2C [30–32], which represents a homogeneous monolithic phase with white extended inclusions of lamellar morphology (Figure 2b).

3.1. Morphological forms of carbide inclusions

Deep etching of polycarbide quasi-eutectic revealed a variety of morphological forms of carbide inclusions (Figure 3): globular and ellipsoidal (Figure 3a), vixers or filamentous nanocrystals (Figure 3b), and lamellar (Figure 3c), which were previously revealed by surface etching (Figure 2b).

Chemical analysis showed that the globular and filamentous inclusions (Figure 3a and 3b) correspond to the chemical composition of FeC monocarbide (18.0% C) and ε-carbide Fe_2C (9.6% C), while the ledeburite framework is a polycarbide quasi-eutectic including a continuous series of solid solutions based on FeC carbides (18.0% C), Fe_3C_2 (12.5% C), Fe_2C (9.6% C), Fe_5C_2 (8.0% C), and Fe_3C (6.67% C). Figure 4a shows the local chemical composition of carbide inclusions of different morphologies: 4b - 10.21%C (phase 1 Fe_2C); 4c - 11.0%C (phase 2 Fe_2C); 4d - 17.11%C (phase 3 FeC); 4e - 7.38%C (phase 4 Fe_5C_2), including the carbon content in the carbide peritectoid (Figure 4e). The platelike inclusions correspond to the chemical composition of ε-carbide Fe_2C (9.6% C). Figure 5a shows the local chemical composition of lamellar and globular carbide inclusions: 5b - 10.23%C (phase 1 Fe_2C); 5c - 9.84%C (phase 2 Fe_2C).

Further investigations showed that globular and filamentous nanocrystals of carbide inclusions (Figure 3a and 3b) are nucleated crystals of FeC (18.0% C) monocarbide and ε-carbide Fe_2C (9.6%C),

Figure 2
Fine structure of ledeburite eutectoid in eutectic white cast iron. (a) Cast structure of lamellar troostite in the phase cell of ledeburite framework (×100000). (b) Homogeneous monolithic structure of eutectoid colonies after completion of peritectoid transformation during isothermal holding for 36 h at 330°C ± 10°C (×30000)

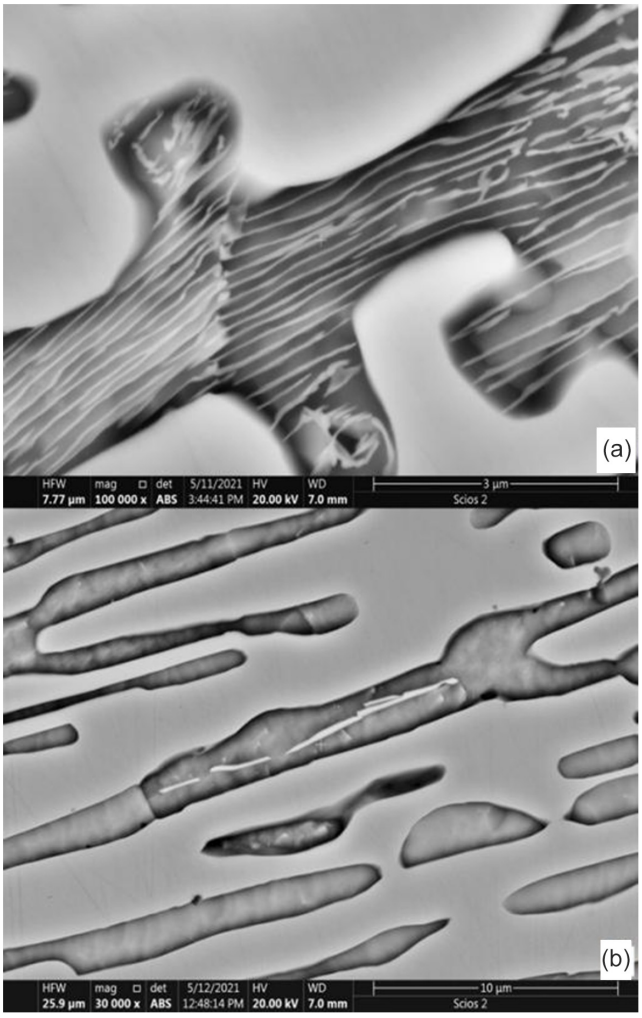

and lamellar carbide inclusions (Figure 2b and 3c) are either formed lamellar single crystals based on ε-carbide Fe_2C (9.6% C) or composite lamellar crystals based on co-crystallization of ε-carbide Fe_2C (9.6% C) and monocarbide FeC (18.0% C).

3.2. Homogeneous crystallization of single crystals of *ε*-carbide Fe_2C

Figure 6 shows the main stages of the process of nucleation and growth of lamellar single crystals of ε-carbide Fe_2C on homogeneous crystallizations centers (Figure 4). Nucleation starts with the formation of globular or spherical nuclei (Figure 3a and 6a, item 1), with diameters from 20 to 40 nm, which during growth form vixers or filamentous nanocrystals (Figure 3b and 6a, item 2) with diameters up to 50 nm and average lengths from 100 to 300 nm. In the process of further crystallizations, vixers aggregate into flat crystalline packages (Figure 6a, item 3), which crystallize into extended platelike single crystals of ε-carbide Fe_2C (Figures 2b, 3c, and 6b) during growth intensification. The considered growth

Figure 3
Morphological shapes of carbide inclusions in phase cells. (a) Globular and ellipse-shaped (×100000); (b) vixers or filamentous nanocrystals (×100000). (c) Lamellar (×50000)

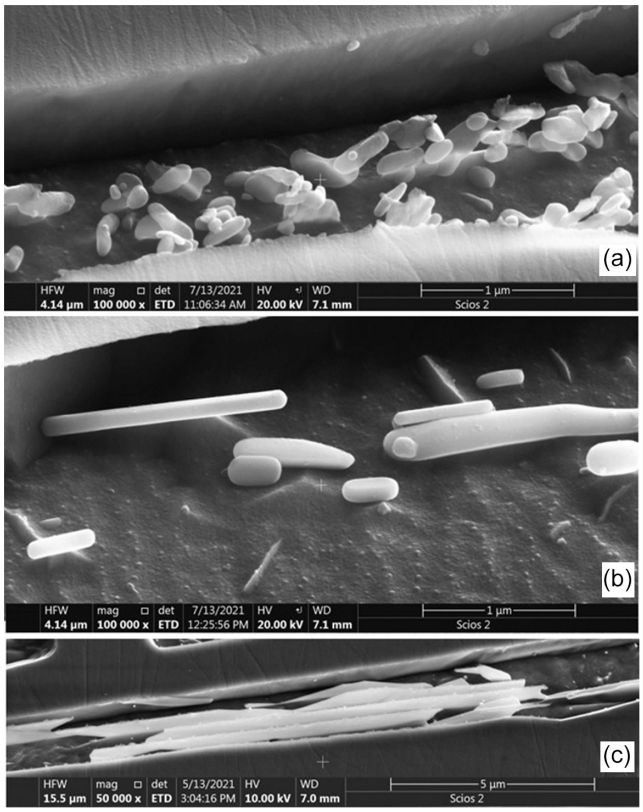

process of single crystal of ε-carbide Fe_2C in the form of isolated inclusions confirms its stoichiometric composition as a chemical compound or berthollide.

3.3. Homogeneous crystallization of FeC monocarbide single crystals

Figure 7 shows the main stages of nucleation and growth of homogeneous single crystals of FeC monocarbide (Figure 4).

Crystallization of FeC monocarbide begins with the nucleation of spherical nuclei with diameters from 50 to 100 nm (Figure 7a, item 1) on microroughnesses of the inner surface of the phase cell with subsequent growth to the inclusion of an elongated ellipsoid of rotation (Figure 7, item 2), which subsequently forms the FeC monocarbide crystal body with a smooth crystallization front (Figure 7, item 3). At further growth of FeC monocarbide monocrystal, the smooth crystallization front on its surface changes to a cellular crystallization front (Figure 7, item 4), which forms a two-dimensional crystalline nanofilm of FeC monocarbide (Figure 7, item 5). This fact is confirmed by the presence of a thin interface on the crystal surface, which is covered by the nanofilm during its movement along the crystal surface (Figure 7a, item 5, yellow arrow) and the formation of a two-layer flat crystal (Figure 7b, item 5, yellow arrow). As further growth progresses, the crystal configuration begins to acquire a distinctly dendritic structure (Figure 7b).

Figure 8 shows different morphological forms of the two-dimensional crystalline FeC monocarbide nanofilm in the form of flat, extended, ribbon-shaped inclusions forming dense crystal

Figure 4
Spectral analysis of carbon content. (a) In globular and cylindrical carbide inclusions (phases by the yellow arrow). (b) 10.21% C (phase 1 Fe_2C). (c) 11.0% C (phase 2 Fe_2C). (d) 17.11% C (phase 3 FeC). (e) 7.38% C (phase 4 Fe_5C_2)

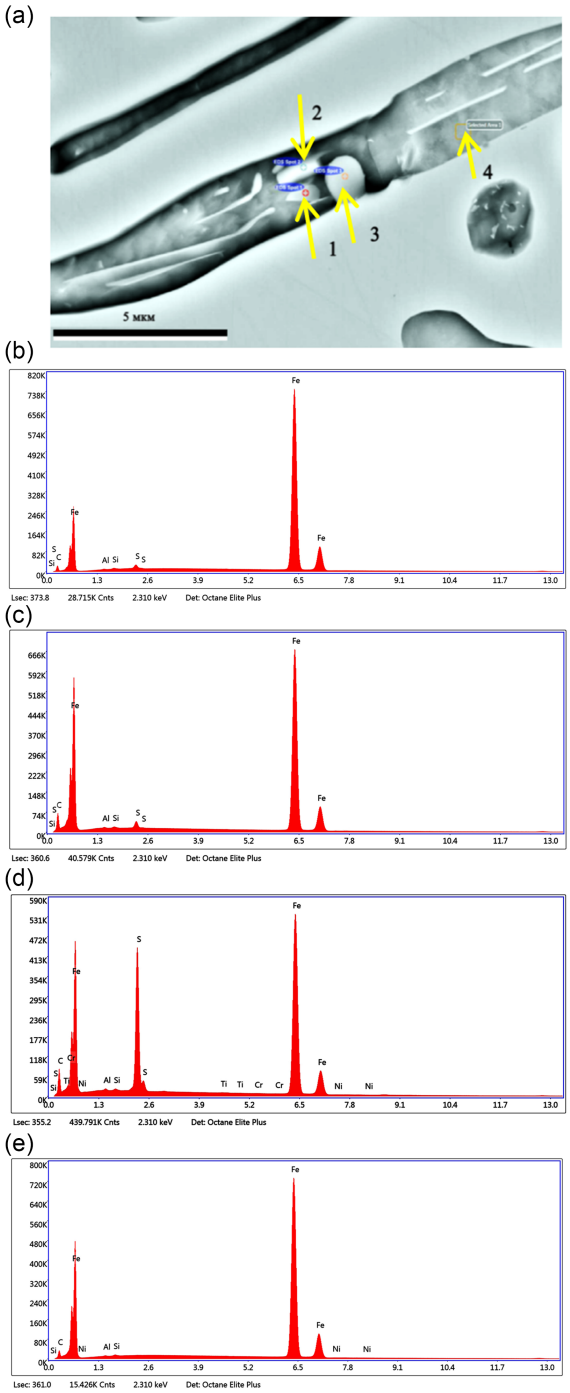

associations. The two-dimensional crystalline nanofilm of FeC monocarbide has an incredible and unusual property – it is matte-transparent, and the contours of the structures behind the nanofilm can be clearly seen through it. Moreover, it is so elastic that it envelops neighboring carbide inclusions (Figure 8a and 8b). There is also observed (Figure 8c) the separation of packets of two-dimensional crystalline nanofilm of monocarbide FeC.

Figure 5
Spectral analysis of carbon content. (a) In globular and lamellar carbide inclusions (phases in yellow arrow); (b) 10.23% C (phase 1 Fe_2C); (c) 9.84% C (phase 2 Fe_2C)

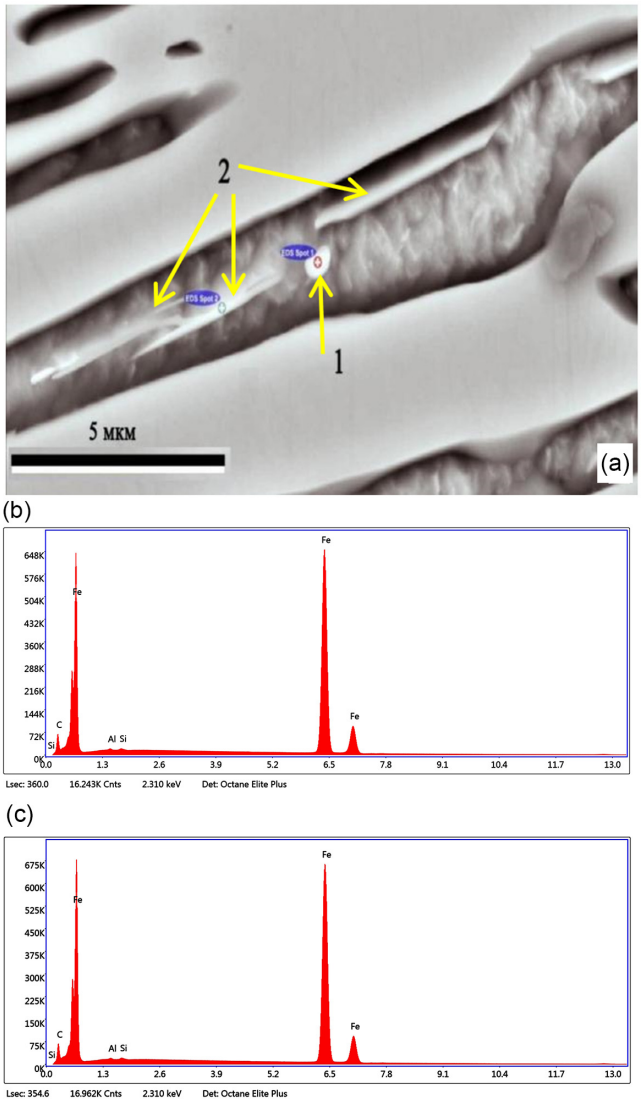

Figure 6
Process of nucleation and growth of lamellar single crystals of ε-carbide Fe_2C in phase cells. (a) Main stages of nucleation and growth (1-globular nucleation, 2-growth of vixers from globular crystallization center, 3-growth of vixers into flat crystal packages), ×60000. (b) Formed extended lamellar single crystals of ε-carbide Fe_2C, ×50000

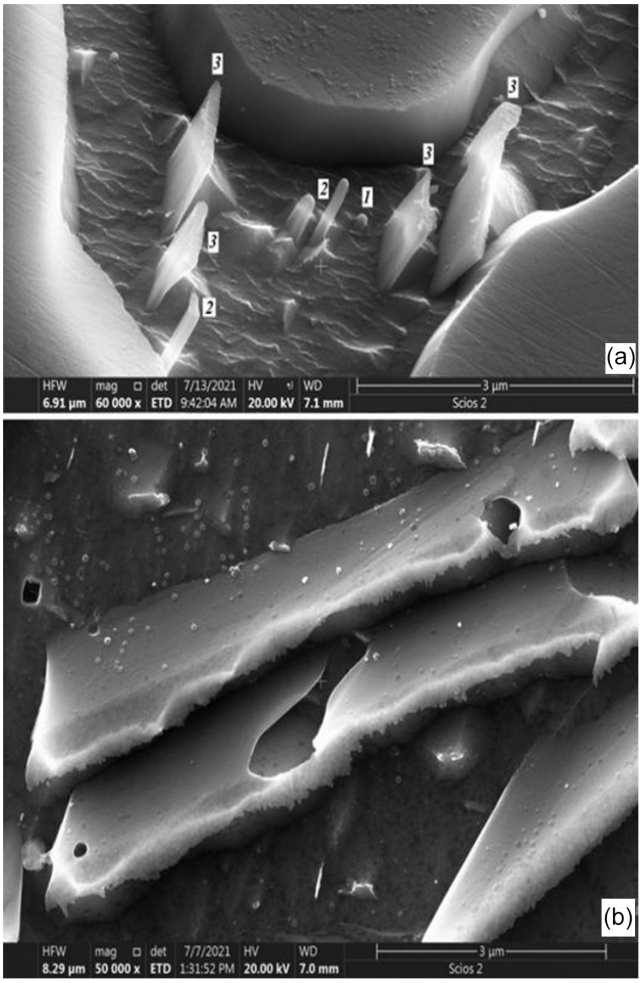

The obtained experimental data fully confirm the theoretical studies of the crystallographic structure of FeC monocarbide performed by [13, 14].

Using systematic ab initio calculations, they theoretically discovered energetically stable two-dimensional allotropes of FeC monocarbide characterized by planar hypercoordination chemical bonding, respectively: tetragonal FeC monocarbide (t-FeC) and orthorhombic FeC monocarbide (o-FeC). Allotropes of FeC monocarbide are the first example of two-dimensional monolayers with simultaneously pentacoordinated carbon bonds and seven-coordinated iron atom bonds in known iron-carbon materials.

In fact, Figures 7b and 8 show the homogeneous crystallization of two-dimensional monolayers of FeC monocarbide allotropes in the form of translucent extended and elastic crystalline nanofilms. Based on the fine structural organization of the detected nanofilms, they are completely inert to the nitric acid etching process, which indicates their high chemical resistance in addition to the results of theoretical calculations, which showed [13, 14] that two-dimensional monolayers of FeC monocarbide allotropes have significant dynamic, mechanical, and thermal stability and, as was found experimentally above, have high elasticity or plastic properties.

3.4. Heterogeneous crystallization of FeC monocarbide single crystals

In addition to homogeneous crystallization of two-dimensional monolayers of FeC monocarbide allotropes on their own nuclei, heterogeneous crystallization of FeC monocarbide allotropes on the inner surfaces of phase cell microrelief elements was also found, which further confirms the truth of Dong et al.'s and other's theoretical calculations [13, 14]. Figure 9 shows multiple elements of heterogeneous crystallization of FeC monocarbide allotrope nanofilms on different surfaces of the phase cell.

Figure 7
Nucleation and growth of homogeneous FeC monocarbide monocrystal. (a) Initial stage of FeC monocarbide crystal development (×100000). (b) Cross section of FeC monocarbide crystal body with film-cellular growth surfaces (×100000); (1) globular crystallization center; (2) growth of crystallization center in the form of an elongated ellipsoid of rotation; (3) FeC monocarbide crystal body; (4) cellular crystallization front; (5) two-dimensional crystalline nanofilm of FeC monocarbide

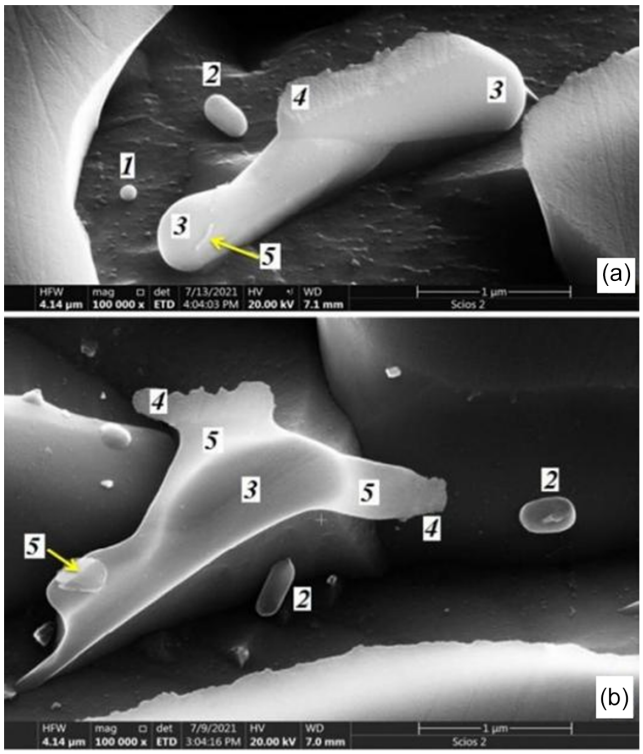

In Figure 9a and 9b, the two-dimensional FeC monocarbide allotrope nanofilm crystallizes on different surfaces of protruding microroughness elements (yellow arrow, microrelief elements; blue arrow, two-dimensional crystalline FeC monocarbide allotrope nanofilm). The FeC monocarbide allotrope nanofilm is matte-transparent, and the darker elements of the microroughnesses of the carbide surface of the phase cell shine through it.

In Figure 9c and 9d, the two-dimensional FeC monocarbide allotrope nanofilm tightly envelops the surfaces of the protruding microroughness elements (yellow arrow, microrelief elements; blue arrow, FeC monocarbide two-dimensional crystalline allotropes nanofilm). The FeC monocarbide allotrope nanofilm is matte-transparent, and darker elements of microroughnesses of the carbide surface of the phase cell shine through it. It should be noted that the elasticity of the FeC monocarbide allotrope nanofilm appears only after etching, when the solid solution based on ε-carbide Fe_2C, into which the nanofilm grew during its growth, is completely dissolved by nitric acid in the phase cell. Once the solid solution is removed, the nanofilm loses its stability and envelops the underlying microrelief surface of the phase cell, which can be clearly seen in Figure 9d. In Figure 9a and 9b, the upper part of the nanofilm protruding above the surface of the facet on which it grows is short and maintains its rigidity and hence its vertical position.

Figure 8
Morphological shapes of two-dimensional crystalline nanofilm of FeC monocarbide allotropes. (a, b) ×50000. (c) ×30000

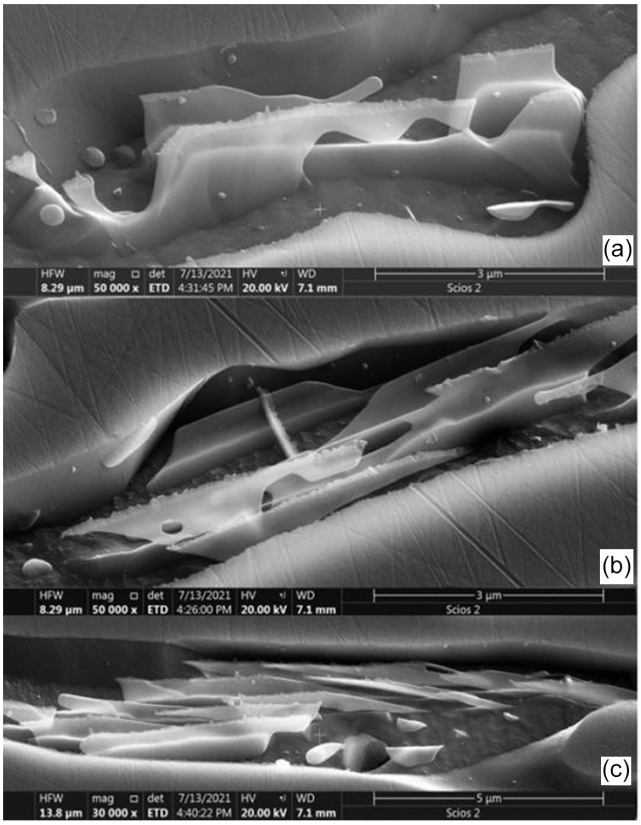

3.5. Co-crystallization of FeC monocarbide on *ε*-carbide Fe_2C substrates

Figure 10 shows the co-crystallization of FeC monocarbide on ε-carbide Fe_2C substrates. As established by the present studies, crystallization of the FeC monocarbide allotrope nanofilm starts either on single voxels (Figure 10a, item 1) or on lamellar packets (Figure 10b) of ε-carbide Fe_2C. The FeC monocarbide allotrope nanofilm is so transparent that the ε-carbide Fe_2C vixer is completely visible through the nanofilm covering it (Figure 10a, item 1).

Longer allotrope nanofilm of FeC monocarbide loses stability after etching and envelops the structural elements of the phase cell (Figure 10b, item 2). Shorter FeC monocarbide allotrope nanofilm retains rigidity and vertical position with a cellular crystallization front (Figure 10b, item 3).

3.6. Crystallization conditions of FeC monocarbide and *ε*-carbide Fe_2C

The considered crystallization processes of FeC monocarbide and ε-carbide Fe_2C are determined by the following conditions.

3.6.1. Dispersive solidification

After completion of peritectoid transformation [30–32], a supersaturated thermodynamically non-equilibrium solid solution based on ε-carbide Fe_2C is formed (Figure 11), which undergoes decomposition by the mechanism of dispersion solidification with

Figure 9
Multiple elements of heterogeneous crystallization of nanofilms of FeC monocarbide allotropes. (a, b) growth of the nanofilm on the lateral surface, (x50000). (c, d) enveloping the surface of protruding elements, (x60000); yellow arrow – microrelief elements; blue arrow – two-dimensional crystalline nanofilm of FeC monocarbide allotropes

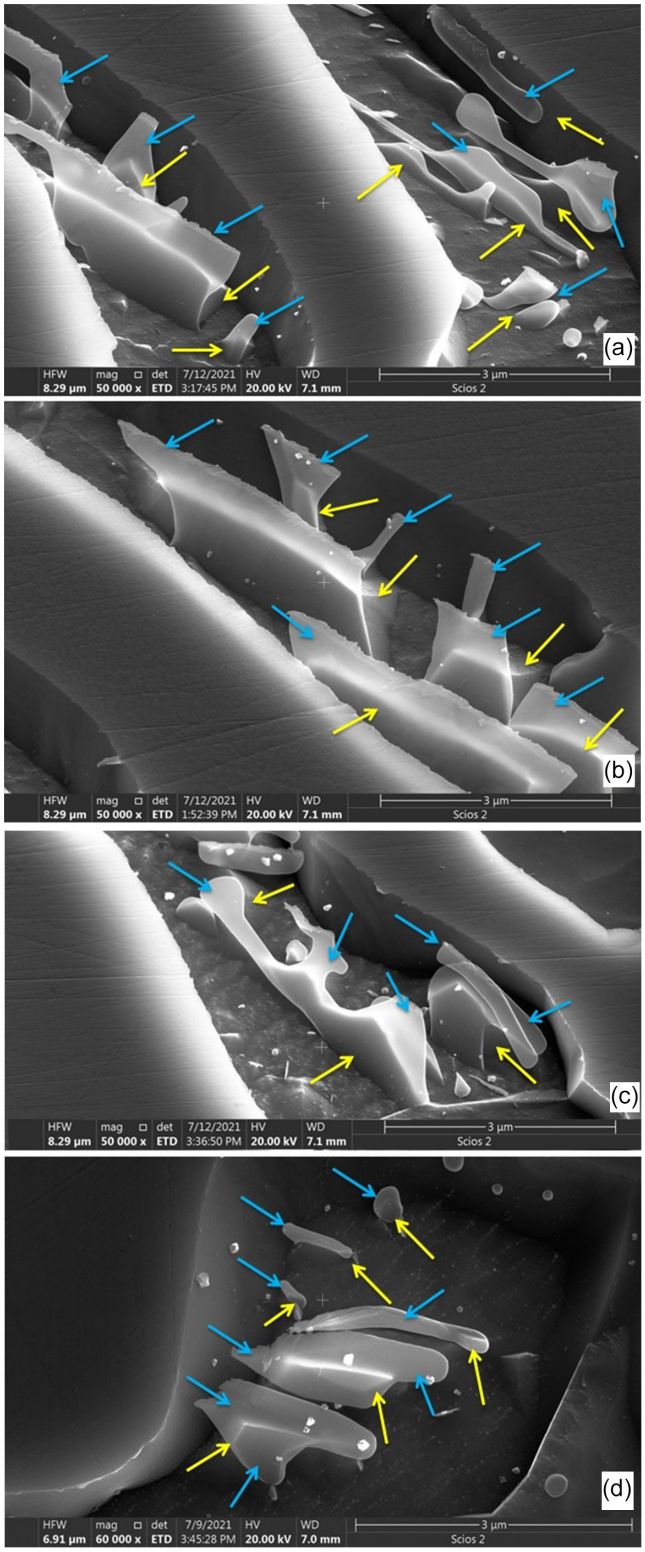

Figure 10
Development and growth of nanofilm crystals of FeC monocarbide allotropes on ε-carbide Fe_2C substrates. (a) Co-crystallization with vixers (×100000). (b) Co-crystallization with plate packets (×100000); (1) vixer substrate of ε-carbide Fe_2C; (2) two-dimensional crystalline nanofilm of FeC monocarbide allotropes; (3) cellular crystallization front of FeC monocarbide allotropes nanofilm

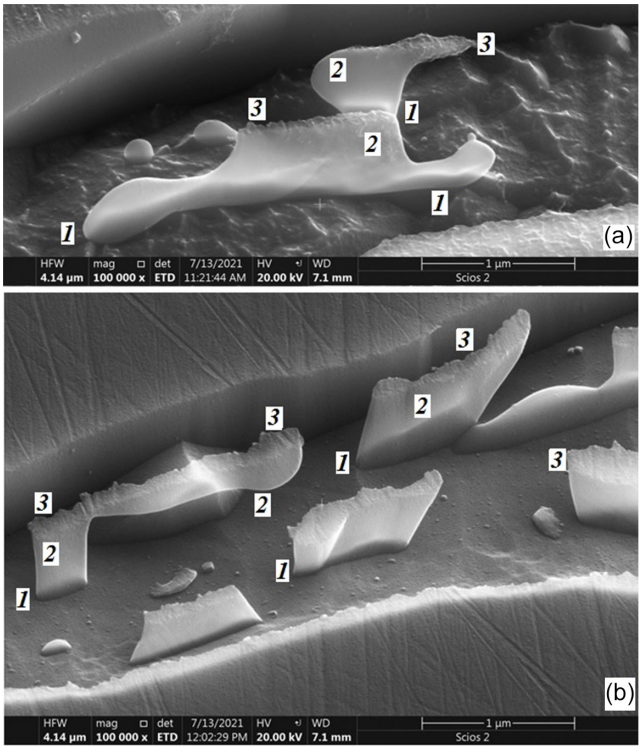

the release of the phase of carbide nanocarbide nano-inclusions of FeC monocarbide and ε-carbide Fe_2C with a size range of 20–40 nm (Figure 3a).

3.6.2. Isovalent isomorphism

Numerous studies of the carbon content in ledeburite of white cast iron (Figures 11 and 12) have shown that its composition does not correspond to the generally accepted carbon content corresponding to cementite Θ-Fe_3C (6.67%C). Chemical composition by carbon in all carbide phases of ledeburite is gradient and varies in wide ranges, which correspond to the carbon content of the following series of carbides: FeC (18.0% C), Fe_3C_2 (12.5% C), Fe_2C (9.6% C), Fe_7C_3 (8.0% C), Fe_5C_2 (8.0% C), Fe_3C (6.67% C), and Fe_4C (5.0% C). The chemical analysis revealed the following features of carbon distribution in the ledeburite carbide structures of eutectic white cast iron after isothermal annealing: average carbon content in the carbide framework of ledeburite - 12.0 . . . 14.0% C (Figure 12a and Figure 12b); on the surfaces of phase cells - minimum 2.0...4.95% C (Figure 11b, Figure 12a, Figure 12b), maximum 5.14 . . . 8.68% C (Figure 11a, Figure 11b, Figure 12b); carbide inclusions of different morphology - 15.0 . . . 23.0% C. There is a rather simple explanation for this phenomenon.

The work of Russian scientists Barinov [33] had shown that all structural models of iron-based carbide phase can be summarized in the "average" model with a finite number of iron and carbon atoms

Figure 11
Carbon content in the carbide phases of ledeburite after annealing and etching: (a) surface and (b) deep

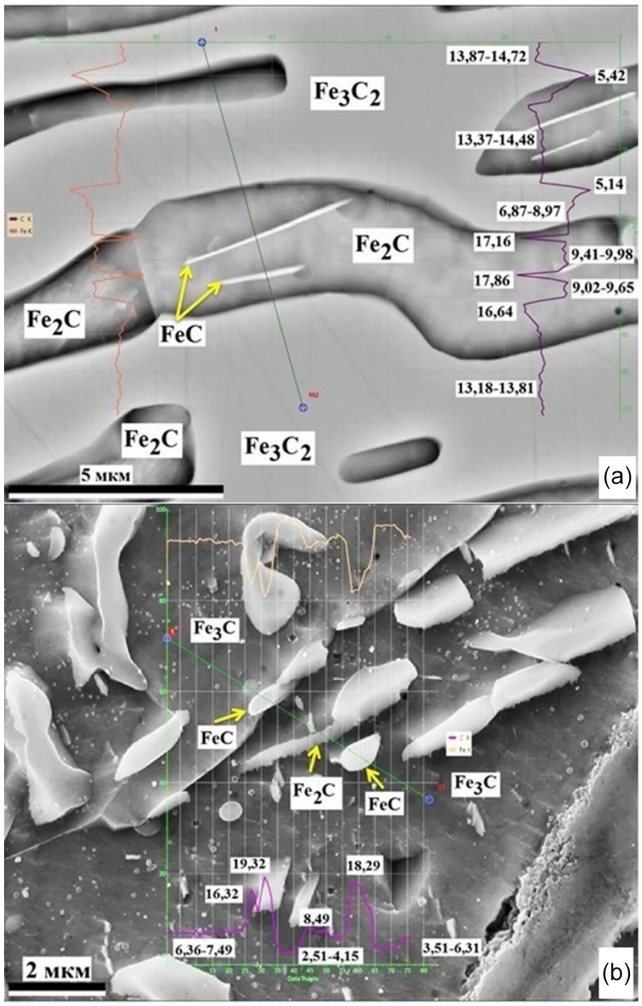

Figure 12
Carbon content in carbide phases after annealing and deep etching: (a) troostite and (b) ledeburite phase cell

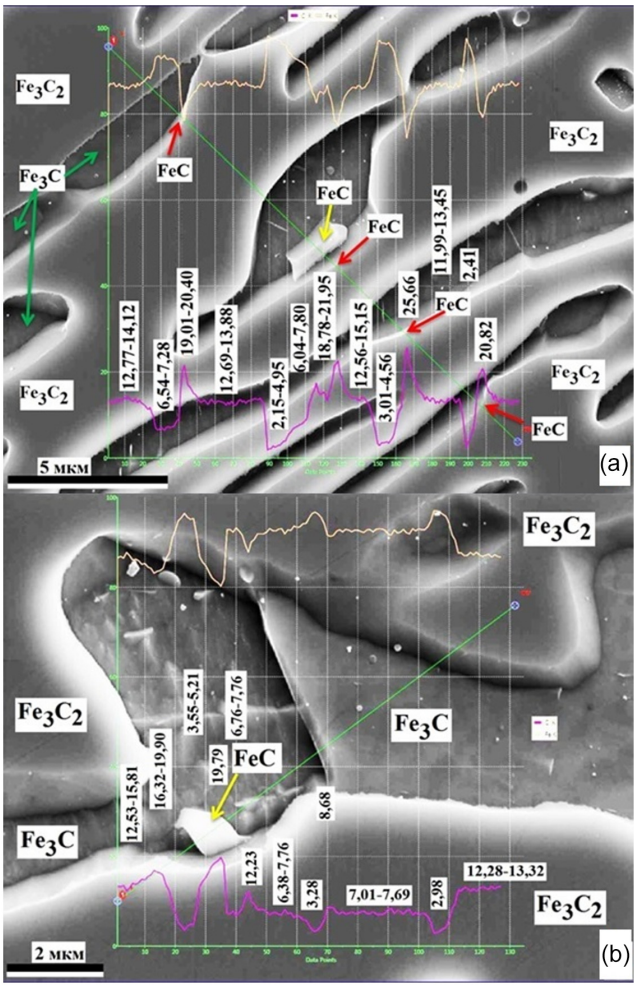

$n_{Fe} = 40$ and $n_C = 24$, localized in the space group Pnma on seven and five crystallographic non-equivalent positions of the rhombic cell, respectively. For example, in such a universal cell, the cementite phase Θ-Fe_3C corresponds to 25% and the Hegg carbide phase χ-Fe_5C_2 <44% of the maximum allowed number of iron and carbon atoms. In the framework of this model [33], carbon atoms do not replace the iron atoms of the matrix but are located in the gaps between them. The dissolving carbon atoms enter the gaps between the matrix iron atoms (internodes), statistically occupying a new position not previously occupied. Since with increasing carbon concentration in the alloy, the same carbon atoms with the same ionic radius and valence are added to the sublattice of iron as a solvent without changing the electroneutrality of the crystal lattice of the solid solution, this type of isomorphism can be defined as isostructural isovalent isomorphism.

A consequence of the isostructural character of carbide phases is the universality of any carbide surface as a coherent surface for the nucleation of crystallization centers during dispersion solidification, for example, crystallization centers are formed on any carbide surface: on the phase cell surface (Figures 3a, 7a), on the surface of ε-carbide Fe_2C inclusion packets (Figure 6b), and on the surface of FeC monocarbide allotrope nanofilms (Figures 8a, 9b).

Consequently, the carbide phases in white cast iron can be characterized as a single isomorphic and isostructural quasi-carbide solid solution, which structurally crystallizes in the form of heterogeneous carbide phases as a quasi-eutectic [30–32], in which the carbon content is free to vary widely without identifying the carbide phases proper as chemical compounds. In general, this structural organization can be briefly characterized as a polycarbide with a gradient crystal lattice of solid solutions corresponding in carbon concentration to one or another carbide. Moreover, FeC monocarbide and ε-carbide Fe_2C are chemical compounds with stoichiometric composition, since only they crystallize in the form of isolated inclusions. The other carbides are non-stoichiometric compounds. Based on the data obtained, the author has constructed a FeC diagram that takes into account carbide transformations to the right of the cementite line [30–32].

Consideration of non-stoichiometric compounds of iron carbides as solid solutions of excess atoms of components in the basic substance [30–32] allows us to represent non-stoichiometry as the ability of crystalline compounds to dissolve their own components, that is, iron-based carbide phases are able to dissolve carbon. Consequently, carbon should be freely redistributed within the iron sublattice without changing the carbide's own lattice and forming one or another type of solid solution. Thus, the carbide phase is a solid

solution for the introduction of the second kind. This fact is proved in the studies of Russian scientists [34] and [35], in which it is shown that the redistribution of unbound carbon in the iron sublattice of carbides occurs in four types of pores: "normal" octahedral and prismatic, as well as "distorted" octahedral and prismatic. This leads to an increase in entropy and a decrease in the free energy of carbides, which is characteristic of the behavior of carbon in solid solution, which was also established by [13, 14], whose work proved that the high adsorption capacity of the o-FeC and t-FeC allotropes also explains the high carbon content of iron carbides up to 23.0% C, which during cooling of the high-carbon carbide melt is actively adsorbed on the monolayers of the crystal lattice of crystallizing FeC monocarbide, forming high-carbon solid solutions. Dong et al. and others [13, 14] also showed that monolayers of o-FeC and t-FeC allotropes have very high thermal stability and can maintain their structural integrity up to 2000 K. The following conclusion can be drawn from the obtained data – FeC monocarbide is the most thermally stable and thermodynamically stable iron carbide from the whole known line of iron carbides.

The most significant result of the present studies is the principal possibility of developing a technology for obtaining and extracting (electrolytic dissolution) from the eutectic of white cast iron the crystalline phases of FeC monocarbide and ε-carbide Fe_2C for in-depth studies, which cannot be obtained by other methods [1–15, 36, 37].

4. Conclusion

1) The previously unknown process of homogeneous and heterogeneous crystallization of FeC iron monocarbide and its co-crystallization with ε-carbide Fe_2C from a supersaturated solid solution based on ε-carbide Fe_2C or polycarbide quasi-eutectic has been investigated.
2) Crystallization of two-dimensional monolayers of FeC monocarbide allotropes in the form of translucent extended and elastic crystalline nanofilms has been experimentally proved.
3) The carbide phases in white cast iron can be characterized as a single isomorphic and isostructural quasi-carbide solid solution, which structurally crystallizes as a mixture of carbide phases as a quasi-eutectic, in which the carbon content is free to vary widely without identifying the carbide phases proper.
4) The decomposition product of the lamellar eutectoid as a result of peritectoid transformation during isothermal annealing is a polycarbide with a gradient crystal lattice of solid solutions corresponding in carbon concentration to one or another carbide.
5) Crystallization of FeC monocarbide and ε-carbide Fe_2C phases in the process of dispersion solidification of solid carbide solution on the basis of ε-carbide Fe_2C in the process of isothermal annealing gives a fundamental possibility to develop the technology of their extraction (e.g., by electrolysis) from the matrix of white cast iron for in-depth studies.
6) Chemical analysis showed that globular and filamentous inclusions correspond to the chemical composition of FeC monocarbide (18.% C) and ε-carbide Fe_2C (9.6% C), and the ledeburite framework is a polycarbide quasi-eutectic including a continuous series of solid solutions based on carbides FeC (18.0% C), Fe_3C_2 (12.5% C), Fe_2C (9.6% C), Fe_5C_2 (8.0% C), and Fe_3C (6.67% C). Plate inclusions correspond to the chemical composition of ε-carbide Fe_2C (9.6% C).
7) The process of nucleation and growth of lamellar ε-carbide Fe_2C single crystals and two-dimensional film crystals of FeC monocarbide allotropes starts with the formation of globular or spherical nuclei, with diameters from 20 to 40 nm, which in the process of growth form vixers or filamentous nanocrystals with diameters up to 50 nm and average lengths from 100 to 300 nm.

Ethical Statement

This study does not contain any studies with human or animal subjects performed by the author.

Conflicts of Interest

The author declares that he has no conflicts of interest to this work.

Data Availability Statement

Data is available upon reasonable request from the corresponding author.

Author Contribution Statement

Sergey Vasilyevich Davydov: Conceptualization, Methodology, Validation, Formal analysis, Investigation, Resources, Data curation, Writing – original draft, Writing – review & editing, Visualization, Supervision, Project administration.

References

[1] Lemire, R., Palmer, D. A., Taylor, P., Urs, B., Claude, M., & Osamu, T. (2013). *Chemical thermodynamics of iron, Part 1 13a* (OECD Nuclea Energy Agency Date Banc (Ed.), Vol. 13a). France: OECD Publications.
[2] Lemire, R., Palmer, D. A., Taylor, P., & Schlenz, H. (2020). *Chemical thermodynamics of iron, Part 2 13b* (OECD Nuclea Energy Agency Date Banc (Ed.), Vol. 13b). France: OECD Publications.
[3] Cahn, R. W., & Haasen, P. (1983). *Physical metallurgy* (4th, ed., p. 4911). Netherlands: North-Holland Physics Publishing.
[4] Laughlin, D. E., & Hono C. (2014). *Physical metallurgy* (5th ed., p. 2960). USA: Elsevier.
[5] Bahgat, M. (2006). Technology of iron carbide synthesis. *Journal of Materials Science & Technology*, *22*(03), 423–432.
[6] Balfour, W. J., Cao, J., Prasad, C. V. V., & Qian, C. X. W. (1995). Electronic spectroscopy of jet-cooled iron monocarbide. The 3Δi←3Δi transition near 493 nm. The Journal of Chemical Physics, 103(1), 4046–4051.
[7] Shim, I., & Gingerich, K. A. (1999). All electron ab initio investigations of the electronic states of the FeC molecule. *The European Physical Journal D - Atomic, Molecular and Optical Physics*, *7*(2), 163–172.
[8] Brugh, D. J., & Morse, M. D. (1997). Optical spectroscopy of jet-cooled FeC between 12 000 and 18 100 cm—1. *The Journal of Chemical Physics*, *107*(23), 9772–9782.
[9] Aiuchi, K., & Shibuya, K. (2001). The electronic spectrum of jet-cooled FeC in the visible region. *Journal of Molecular Spectroscopy*, *209*(1), 92–104.
[10] Steimle, T. C., Virgo, W. L., & Hostutler, D. A. (2002). The permanent electric dipole moments of iron monocarbide, FeC. *The Journal of Chemical Physics*, *117*(4), 1511–1516.
[11] Allen, M. D., Pesch, C., & Ziurys, M. (2009). The pure rotational spectrum of FeC (X3Δi). *The Astrophysical Journal*, *472*(1), L57–L69.
[12] Liu, X. W., Zhao, S., Meng, Y., Peng, Q., Dearden, A. K., Huo, C. F., . . . , & Wen, X. D. (2016). Mössbauer spectroscopy of iron carbides:

From prediction to experimental confirmation. *Scientific Reports*, *6*, 26184–26194.

[13] Fan, D., Lu, S., & Hu, X. (2018). Two-dimensional iron monocarbide with planar hypercoordinate iron and carbon. *Journal of Physical Chemistry C*, *122*, 15118–15124.

[14] Fan, D., Chen, C., Lu, S., Li, X., Jiang, M., & Hu, X. (2020). Highly stable two-dimensional iron monocarbide with planar hypercoordinate moiety and superior Li-ion storage performance. *ACS Applied Materials & Interfaces, 12*(27), 30297–30303.

[15] Larionov, K. V. (2022). Theoretical study of structural, electronic and magnetic properties of new low-dimensional compounds on the basis of transition metals/Dis . . . k-ta phys. mat. sciences. Speciality 1.3.8 - Physics of condensed state. //Moscow: Technological Institute of superhard and new carbon materials, 115.

[16] Ngqase, M., & Pan, X. (2020). An overview on types of white cast irons and high chromium white cast irons. *Journal of Physics: Conference Series, 1*, 1495–1508.

[17] Trepczyńska-Łent, M. (2013). Directional solidification of ledeburite. *Archives of Foundry Engineering*, *13*(3), 101–106.

[18] Park, J. S., & Verhoeven, J. D. (1996). Directional solidification of white cast iron. *Metallurgical and Materials Transactions*, *27*(8), 2328–2337.

[19] Chemicals and Materials. (2023). Malleable Iron Castings Market, Global Outlook and Forecast 2023–2029. 118.

[20] Abdulla, H. H., Ibraheem, A. A., & Khudhair, A. A. A. (2022). Production of ductile iron using inside-mold treatment technique. *Iraqi Journal of Industrial Research, 9*(2), 22–30.

[21] Sukhanov, D. A., Arkhangelsky, L. B., & Plotnikova, N. V. (2017). Damascus steel ledeburite class. *IOP Conference Series: Materials Science and Engineering, 4th International Conference on Competitive Materials and Technology Processes*, *175*, 1–7.

[22] Vasyunina, N. V., Dubova, I. V., Druzhinin, K. E., & Gilmanshina, T. R. (2023). Ferrum extraction in cast iron via reduction smelting of red mud. *CIS Iron and Steel Review*, *25*, 115–121.

[23] Sukhanov, D. A., & Arkhangelsky, L. B. (2017). Formation of eutectic carbides in the structure of high-purity white cast iron in the forging process. *Materials Sciences and Applications*, *08*(05), 351–360.

[24] Sukhanov, D. A., Arkhangel'skii, L. B., & Plotnikova, N. V. (2018). Mechanism of Fe2C type eutectic carbide formation within damascus steel structure. *Metallurgis*, *62*, 261–269.

[25] Santos, T., Chaubet, D., Botelho, T. D. S., Poize, G., & Bacroix, B. (2023). Analysis of the microstructural features of phase transformation during hardening processes of 3 martensitic stainless steels. *Metallurgical Research Technology*, *120*(117), 1–16.

[26] Cios, G., Winkelmann, A., Nolze, G., & Tokarski, T. (2023). Mapping of lattice distortion in martensitic steel—Comparison of different evaluation methods of EBSD patterns. *Ultramicroscopy*, *253*(6), 113824–113830.

[27] Pereira, H. B., Echeverri, E. A. A., Centeno, D. M. A., de Souza, S. D. S., Bauri, L. F., Manfrinato, M. D., . . . , & Goldenstein, H. (2023). Effect of pearlitic and bainitic initial microstructure on cementite spheroidization in rail steels. *Journal of Materials Research and Technology*, *23*, 1903–1918.

[28] Ribamar, G. G., Escobar, J. D., da Silva, A. K., Schell, N., Ávila, J. A., Nishikawa, A. S., . . . , & Goldenstein, H. (2023). Austenite carbon enrichment and decomposition during quenching and tempering of high silicon high carbon bearing steel. *Acta Materialia*, *247*, 1–11.

[29] Mihailović, M., Patarić, A., & Jordović, B. (2023). Heat treatment featuring the key-parameters of high chromium white cast iron microstructure. *Metallurgical and Materials*, *1*(3), 81–83.

[30] Davydov, S. V. (2020). Low-temperature carbide transformation in pearlite of medium-carbon steels. *Steel in Translation*, *50*(9), 639–647.

[31] Davydov, S. V. (2021). Temperature metastable perlite in iron-carbon alloys. *Steel in Translation*, *51*(11), 805–813.

[32] Davydov, S. V. (2020). Phase equilibria in the carbide region of the iron-carbon phase diagram. *Steel in Translation*, *50*(12), 888–896.

[33] Barinov, V. A., Protasov, A. V., & Surikov, V. T. (2015). Investigation of mechanosynthesized χ-Hagg carbide. *Physics of Metals and Metallurgy*, *116*(8), 835–845.

[34] Okishev, K. Y., & Mirzaev, D. A. (2003). About possible positions of carbon atoms in the lattice of cementite. *Physics of Metals and Metallurgy*, *96*(3), 75–78.

[35] Medvedeva, N. I., Karkina, L. E., & Ivanovsky, A. L. (2003). Influence of the effects of atomic disorder and non-stoichiometry on the carbon sublattice on the zone structure of cementite Fe3C. *Physics of Metals and Metallurgy*, *96*(5), 16–20.

[36] Avdeev, Y. G., & Kuznetsov, Y. I. (2023). Iron oxide and oxyhydroxide phases formed on steel surfaces and their dissolution in acidic media. Review. *The International Journal of Corrosion and Scale Inhibition*, *12*(2), 366–409.

[37] Li, C.-G., Zhang, J., Zhang, W. Q., Tang, Y. N., Ren, B. Z., & Hu, Y. F. (2017). First-principle study of structural, electronic and magnetic properties of (FeC)n (n = 1–8) and (FeC)8TM (TM = V, Cr, Mn and Co) clusters. *Scientific Reports*, *7*(1), 17516–17526.

How to Cite: Davydov, S. V. (2024). Crystallization of FeC Iron Monocarbide During Peritectoidal Transformation of the Lamellar Eutectoid of Ledeburite White Eutectic Cast Iron. *Archives of Advanced Engineering Science*. https://doi.org/10.47852/bonviewAAES42022525